materials proceedings

MDPI

Proceeding Paper

Self-Assembling Nano- and Microparticles of Chitosan L- and D-Aspartate: Preparation, Structure, and Biological Activity †

Anna Shipovskaya [1,*], Xenia Shipenok [1], Tatiana Lugovitskaya [2] and Tatiana Babicheva [1]

[1] Institute of Chemistry, Saratov State University, 410012 Saratov, Russia; kshipenok@gmail.com (X.S.); tatyana.babicheva.1993@mail.ru
[2] Institute of New Materials and Technologies, Ural Federal State University, 620002 Ekaterinburg, Russia; tlugovitskaja@mail.ru
* Correspondence: shipovskayaab@yandex.ru
† Presented at the 4th International Online Conference on Nanomaterials, 5–19 May 2023; Available online: https://iocn2023.sciforum.net.

Abstract: The paper considers the processes of formation of chiral nano- and microparticles in solutions of the D-aminoglucan chitosan (CS) in L- and D-aspartic acid (AspA) by means of counterionic condensation of components and stabilization of particles by a polysiloxane shell. The effect of the L- and D-enantiomer of AspA on the structure, size, shape, and zeta potential of nano(micro)particles was studied by IR spectroscopy, dynamic light scattering, and electron and optical microscopy. It was found that chiral particles of CS·L-AspA and CS·D-AspA are non-toxic, hemo- and biocompatible, and also exhibit high growth-stimulating activity for test plants with the best effect for homochiral D-glucan–D-AspA particles.

Keywords: chitosan; aspartic acid; L- and D-enantiomers; nano(micro)particles; chirality; biological activity; growth-stimulating ability

Citation: Shipovskaya, A.; Shipenok, X.; Lugovitskaya, T.; Babicheva, T. Self-Assembling Nano- and Microparticles of Chitosan L- and D-Aspartate: Preparation, Structure, and Biological Activity. *Mater. Proc.* **2023**, *14*, x. https://doi.org/10.3390/xxxxx

Published: 5 May 2023

1. Introduction

CS nano- and microparticles are very promising for use in biomedicine and biotechnology due to their non-toxicity, biodegradability, a wide range of biologically valuable properties, and low cost of raw materials [1–4]. The main properties and application potential of nano(micro)particles of this D-aminoglucan significantly depend on the size, zeta potential, morphological and surface characteristics, including the functionalization of the surface with a protective shell [1,2,4]. The small size of such nano(micro)particles and, accordingly, a large surface area provide a significantly higher antimicrobial and antibacterial activity against various pathogenic bacteria and plant pathogens compared to the original polymer [4,5].

Some publications have noted great prospects for using CS salts with biologically active carboxylic acids and amino acids to obtain nano(micro)particles with improved properties. E.g., CS ascorbate nanoparticles obtained by ionotropic gelation with pentasodium tripolyphosphate were characterized by antioxidant, mucoadhesive, wound healing and antimicrobial properties, which were significantly better than those in comparison with a CS solution in ascorbic acid prepared at the same concentration of both the polymer and acid [6,7]. Nanoparticles based on CS glutamate, aspartate, glycolate and lactate also obtained by ionotropic gelation, but with sodium tripolyphosphate, showed high efficiency when loaded with bovine serum albumin [8]. In this case, the conformation of macrochains and the viscosity of the polymer in the source aqueous acid solution depended significantly on the nature of the organic acid used, which, in turn, affected the dimensional, charge and functional characteristics of the nanoparticles.

We have studied the biological activity of nano(micro)particles of CS L-aspartate formed in the system CS + L-AspA + water at the initial stage of phase separation by the mechanism of counterionic condensation [9]. It was established that the cultivation of *Staphylococcus aureus* 209 P and *Escherichia coli* 113-13 in a nutrient medium with the addition of these particles led to massive death of the bacterial cultures with the highest biocidal effect against gram-positive bacteria. At the same time, in vitro biotesting on the model of cell lines of human dermal fibroblasts and normal keratinocytes, as well as epitheliocytes of the embryonic kidney of the rhesus macaque MA-104, revealed a high biocompatibility of the particles and their ability to accelerate the proliferative activity of these epidermal and epithelial cell cultures. However, dispersions of such nano(micro)particles of CS L-aspartate were kinetically unstable because they form spontaneously due to phase segregation of the polymer substance [10]. In this regard, the task was set to stabilize these nano(micro)particles by forming a protective shell on their surface from pharmacologically active silicon tetraglycerolate. In addition, since the nature of the solvent acid used, including the isomeric forms of such a substance [8,11,12], significantly affects the biological activity of chitosan-containing materials obtained from solutions, not only L-AspA, but also its D-enantiomer was used to form particles.

The purpose of this work was to obtain chiral nano(micro)particles of CS L- and D-asparaginate, functionalize their surface with a protective shell, and evaluate the size characteristics and some biological properties.

2. Experimental Section

2.1. Materials

The following reagents were used: CS with a viscosity average molecular weight of 200 kDa, a degree of deacetylation DD = 82 mol% (Bioprogress Ltd., RF); L-AspA (JSC Bioamid, RF); D-AspA (Vekton Ltd., RF); distilled water; and laboratory-synthesized silicon tetraglycerolate ($Si(OGly)_4$) to the method from Ref. [13]. All reagents were chemical grade and used without further purification.

2.2. Obtaining Nanoparticles

An Atlas reactor (Syrris, England) was used. Distilled water (50 mL) was poured into a round-bottom flask, heated up to 50°C under stirring on a magnetic stirrer at 400 rpm, 0.3 g of CS was added, and the suspension was stirred during 20 min for CS particles to swell. Then, 0.4 g of L- or D-AspA and 50 mL of distilled water were added, stirring was continued under the same conditions for 3 h until the solids were completely dissolved, and filtered through a Schott-160 funnel. 25 mL of the filtered CS solution was taken into a separate round-bottom flask, ~0.08 g of $Si(OGly)_4$ was added, and the mixture was stirred at 50°C for 6 h, as described above. The initial and modified (with a polysiloxane shell) colloidal solutions of CS in L- or D-AspA were stored for no more than t = 2 days and more than t = 300 days, respectively.

2.3. Methods of Examination

Gravimetric measurements were carried out on an Ohaus Discovery analytical balance (USA), weighing accuracy being ±0.01 mg.

pH was measured on a Mettler Toledo Five Easy FE20 pH meter (Germany).

The main characteristics (average diameter (d, nm), proportion of the predominant fraction of particles (Q, %), polydispersity index (P_i), electrokinetic potential (ζ, mV)) of nanoparticles and the conductivity of their aqueous dispersions (χ, mS/cm) were determined by dynamic light scattering (DLS) on complex equipment Zetasizer Ultra Red Label Malvern Panalytical (Great Britain) at 23 ± 2 °C.

IR spectra were recorded on a Bruker Alpha IR Fourier spectrometer equipped with an ATR (ZnSe) attachment in the wavenumber range 500–4000 cm^{-1}. Sample preparation was carried out as follows. The dispersion of nano(micro)particles was placed into a Petri

dish, dried in an air atmosphere at 23 ± 2 °C until an air-dry film was formed for 48 h, and crushed to a powder with a particle size of ~150 μm.

SEM images were taken on a MIRA\\LMU scanning electron microscope (Tescan, CZ) equipped with an energy dispersive detector (EDX) at a voltage of 30 kV and a conducting current of 400 pA. A 5 nm thick gold layer was deposited on each sample using a K450X Carbon Coater (DE). FIB-SEM images were obtained on a Termo Scientific SCIOS 2 electron-ion (two-beam) scanning microscope at an accelerating voltage of 2 kV. A layer of gold was deposited onto each sample on a Jeol JEE-420 vacuum evaporator. During sample preparation for SEM and TEM, a drop of the nano(micro)particle dispersion was applied onto a glass substrate and dried in an air atmosphere for 24 h.

2.4. Study of Biological Properties

Hemocompatibility was assessed in vitro on a model of human erythrocytes under conditions of detection of oxidized hemoglobin forms according to the method from Ref. [14]. Biocompatibility was studied in vitro on the model of cell lines of human dermal fibroblasts and normal keratinocytes, as well as epithelial cells of the embryonic kidney of the rhesus macaque MA-104 [10]. The antimicrobial and antifungal effects were studied in vitro using a daily culture model of rhizospheric bacteria Pseudomonas aureofaciens cultivated in meat-peptone broth (MPB) according to Ref. [9]. Biostimulating activity was tested in vivo for test plants of radish Raphanus sativus and mustard Sinapis Alba. Seeds of these test plants in the amount of 75 pieces were planted in open ground according to traditional methods of agricultural technology and grown for 25 days. Irrigation with the dispersion of nano(micro)particles and water (control) was carried out on the day of planting, then once every 2 days at the rate of the volume of irrigation liquid / volume of bed soil = 0.2. The growth-stimulating effect was assessed by seed germination, as well as by the height and weight of vegetative shoots of the test plants.

In all experiments to assess biological activity, at least three parallel experiments were performed. Statistical data processing was carried out using Statistica 6.0.

3. Results and Discussion

3.1. Preparation and Characterization of Nano(micro)particles of Chitosan L- and D-Aspartate

It has been established that chiral (enantioenriched) salt complexes of CS with L- and D-AspA in aqueous solution exhibit the properties of a partially charge-compensated polyelectrolyte [10,11]. This hydrodynamic behavior indicates the implementation of a mixed polyelectrolyte-ionomer mode, when some of the $HAsp^-$ counterions are in an associated (bound) state with $-NH_3^+$ groups of the macrochain with the formation of ion pairs (Figure 1a). It is thermodynamically not favorable for counterions to be in a free state, and they continue to form ion pairs with $-NH_3^+$ groups of polymer chains (ionomers), while losing in entropy, but gaining in electrostatic energy (Figure 1b).

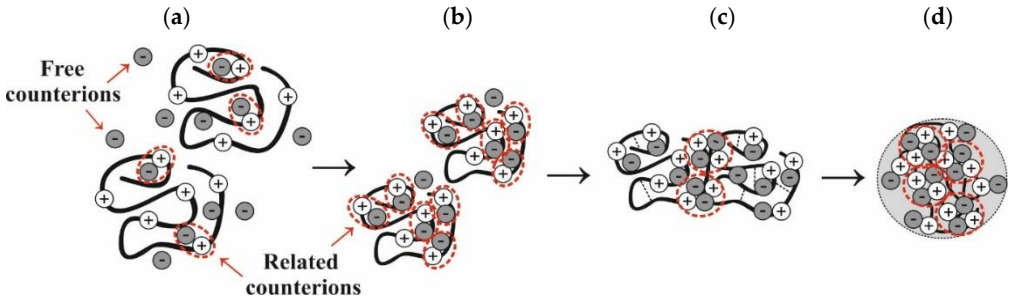

Figure 1. Distribution of free and bound counterions in the CS + AspA + H_2O system during storage: (**a**) polycation with a partially compensated charge, (**b**) ion pairs, (**c**) multiplets, (**d**) phase segregation of the polymer phase in the form of a nanoparticle.

The resulting effective attraction between monomer units contributes to the dipole-dipole interaction of ion pairs and their combination into multiplet structures (Figure 1c). Most likely, the stabilization of the latter occurs through complex ion-ion-hydrogen contacts of ionogenic groups of the CS aspartate macromolecule and the AspA molecule [10]. Multiplets function as physical crosslinks between different polymer chains, which contributes to the compaction of macrocoils and the formation of nanosized nuclei of a new phase (Figure 1d). Upon aggregation of the latter to microand macroparticles, the metastable polymer system is divided into two equilibrium phases: the polymer-rich phase precipitates, the polymer-depleted phase is represented by the supernatant liquid.

To characterize the chiral nano(micro)particles formed in the CS + AspA + water system, we used two complementary methods, namely: DLS and FIB-SEM.

According to DLS, the average size and zeta potential of the particles formed in a freshly prepared aqueous solution of CS in L-AspA were ~1.20 μm and ~38 mV; respectively, those for CS in D-AspA were somewhat smaller, ~0.75 μm and ~36 mV (Table 1). (It should be noted that the effective radius of the macromolecular coil of these salt forms of CS was also larger for CS L-aspartate [11]). EDX analysis showed that the elemental composition of the polymer phase of particles in an air-dry state was represented by 42.95 ± 1.2% carbon, 21.09 ± 0.9% nitrogen, and 35.96 ± 1.0% oxygen. This, as well as the results of Ref. [10], proves that the microparticles are represented by the chiral salt form of the polymer—CS aspartate. The colloidal stability of CS L- and D-aspartate microparticles formed at the initial stage of phase separation of the system under study did not exceed 24–48 h.

Table 1. Physicochemical characteristics of the CS + L-(D-)AspA + water system and size characteristics of chiral particles of chitosan L- and D-aspartate obtained by DLS.

System			*t*, days	χ, mS/cm	Particle Characteristics			
CS salt	Modifier	pH			*d*, nm	*Q*, %	P_i	ζ, mV
CS + L-AspA	–	4.5	–	0.74	1200 ± 300	80 ± 8	0.60 ± 0.25	38 ± 3
	$Si(OGly)_4$	3.6	–	0.73	1500 ± 100	94 ± 2	0.40 ± 0.05	37 ± 2
			14	0.71	1500 ± 100	92 ± 2	0.40 ± 0.05	37 ± 2
			40	0.70	1500 ± 100	90 ± 3	0.40 ± 0.05	37 ± 2
			300	0.73	1200 ± 200	95 ± 4	0.40 ± 0.20	36 ± 1
CS + D-AspA	–	4.5	–	0.70	750 ± 150	94 ± 3	0.90 ± 0.10	36 ± 1
	$Si(OGly)_4$	3.5	–	0.70	1000 ± 100	92 ± 2	0.90 ± 0.20	33 ± 3
			55	0.73	1200 ± 200	76 ± 2	0.50 ± 0.10	35 ± 1
			125	0.68	1500 ± 400	66 ± 2	0.60 ± 0.10	31 ± 1

To eliminate the low aggregative stability of CS L- and D-aspartate particles, their surface was dynamically modified and simultaneously functionalized according to the core–shell type due to electrostatic forces. Pharmacologically active silicon tetraglycerolate was used as a sol–gel precursor for the first time [13]. An analysis of Table 1 shows that the average size of the particles modified with the polysiloxane shell increases somewhat, and their zeta potential remains almost unchanged. The sedimentation stability of the dispersions of modified particles increases significantly. Attention is also drawn to the weak scatter in the conductivity and zeta potential values measured at several storage times of the dispersions, which also indicates the kinetic stability of the system. A slight decrease in the zeta potential of CS·D-AspA microparticles during the storage of dispersions could indicate some deterioration in the quality of the coating or particle aggregation. In general, the particle size and zeta potential of CS·L-AspA particles were somewhat larger than those of CS·D-AspA ones.

The functionalization of the surface of nano(micro)particles was proved by the IR method. In the IR spectra of our CS·L-AspA and CS·D-AspA samples isolated from the corresponding associated systems, all characteristic absorption bands typical of this CS

salt form, which we described in detail in Ref. [10], were observed. The absorption bands of the $Si(OGly)_4$ polycondensation product (ν, cm^{-1}) are also clearly visible: for CS·L-AspA these are 2931 и 2881 (C—H, ν_{as} and ν_s), 1414 (CH_2), 1151, 1024 и 990 (C—O, Si—O—C, Si—O—Si), for CS·D-AspA these are 2921 and 2869 (C—H, ν_{as} and ν_s), 1385 (CH_2), 1148, 1026 and 991 (C—O, Si—O—C, Si—O—Si). The IR spectra of CS·L-AspA and CS·D-AspA indicate the presence of inter- and intramolecular hydrogen contacts in the supramolecular structure of our samples. The most informative for confirming the formation of bonds between the particle surface and their polysiloxane shell can be considered the wave range from 990 to 1150 cm^{-1}, within which, in addition to the absorption bands of vibrations of the precursor polycondensation product, there are also concentrated the absorption bands of deformation vibrations of primary amines associated with the –OH group of the vibration C—O bonds in alcohols and ethers (β–1,4–glucans) and C—O—C, predisposed to intermolecular interaction.

The shape and average diameters of our chiral nano(micro)particles of CS L- and D-aspartate were also studied by FIB-SEM after drying the samples on a glass slide. All nanoparticles had a shape close to spherical (Figure 2). The largest average characteristic effective diameter (largest transverse size) of CS·L-AspA nanoparticles was 17.02 ± 1.25 nm, the smallest was 13.65 ± 1.28 nm, for CS·D-AspA nanoparticles these were 16.25 ± 3.50 nm and 14.84 ± 1.50 nm, respectively. The differences in the sizes of nano(micro)particles determined by DLS and FIB-SEM are typical and are due to different conditions for estimating the dimensional characteristics. E.g., DLS studies were carried out with dispersions of hydrated particles in water, while FIB-SEM studies were carried out with air-dry samples.

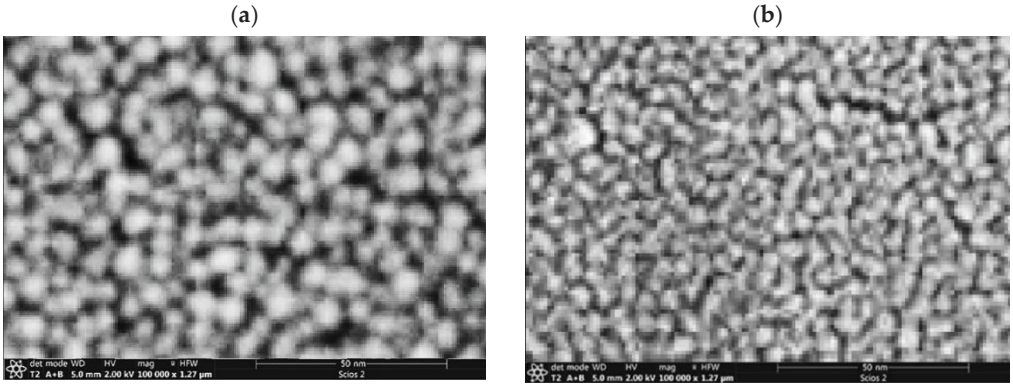

Figure 2. FIB-SEM images of chitosan L- (**a**) and (D-)aspartate (**b**) nanoparticles modified with a polysiloxane shell.

3.1. Biological Properties of Nano(micro)particles of Chitosan L- and D-Aspartate

Special experiments in vitro proved that our chiral nano(micro)particles CS·L-AspA and CS·D-AspA were non-toxic, hemo- and biocompatible.

Experiments in vitro and in vivo revealed that chiral CS·L-(D-)AspA nano(micro)particles are biomimetic of rhizospheric bacteria *Pseudomonas aureofaciens* and could function as an immunizing elicitor, a curing fungicide, and a protective pesticide. This is expressed in their manifestation of high growth-stimulating activity in relation to test plants. E.g., a comparative assessment of the effect of our nano(micro)particles compared with water on the growth-stimulating activity of radish *Raphanus sativus* and mustard *Sinapis alba* in the field showed a significant increase in germination, height and weight of shoots. As compared to irrigation with water, the increase in green mass and, accordingly, the yield with the use of our CS·L-AspA was 32.0 ± 2.9% for radish *Raphanus sativus*, 34.4 ± 3.3% for mustard *Sinapis Alba*, and for CS·D-AspA they were 37.9 ± 5.8% and 39.3 ± 1.6%, respectively. Therefore, the greatest effect of biostimulating activity was observed for the CS·D-AspA sample.

4. Conclusions

Thus, our comprehensive study of solutions of CS in L- and D-AspA revealed the effects of counterionic association (self-organization) with the transition of macromolecules to the ionomeric state and phase segregation of the polymer substance into chiral nano- and microparticles. Optimal conditions for stabilizing particle dispersions by functionalizing their surface with a polysiloxane shell have been developed (pharmacologically active silicon tetraglycerolate was used for the first time as a sol-gel precursor). The results obtained demonstrate the promise of using nano(micro)particles of CS L- and D-aspartate not only in biomedical and pharmacological applications, but also in agriculture for biological control and increasing crop yields. At the same time, there is no negative impact on the environment, since the particle formation process involves the use of biologically active raw materials (CS, AspA) without the use of crosslinking reagents and other biointolerant chemicals. It is noteworthy that our nano(micro)particles of homochiral salt complexes D-glucan·D-AspA exhibit the best biostimulating effect.

Author Contributions: Conceptualization, methodology, writing—original draft preparation A.S.; investigation, data curation, visualization X.S., T.L. and T.B. All authors have read and agreed to the published version of the manuscript.

Funding: This research was funded by a grant from the Russian Science Foundation № 22-23-00320, https://rscf.ru/project/22-23-00320/.

Conflicts of Interest: The authors declare no conflict of interest.

References

1. Chandrasekaran, M.; Kim, K.D.; Chun, S.C. Antibacterial activity of chitosan nanoparticles: A review. *Processes* **2020**, *8*, 1173. https://doi.org/10.3390/pr8091173.
2. Cao, S.; Deng, Y.; Zhang, Le; Aleahmad, M. Chitosan nanoparticles, as biological macromolecule-based drug delivery systems to improve the healing potential of artificial neural guidance channels: A review. *Int. J. Biol. Macromol.* **2022**, *201*, 569–579. https://doi.org/10.1016/j.ijbiomac.2022.01.017.
3. Hembram, K.C.; Prabha, S.; Chandra, R.; Ahmed, B.; Nimesh, S. Advances in preparation and characterization of chitosan nanoparticles for therapeutics. *Artif. Cells Nanomed. Biotechnol.* **2016**, *44*, 305–314. https://doi.org/10.3109/21691401.2014.948548.
4. Hidangmayum, A.; Dwivedi, P. Chitosan based nanoformulation for sustainable agriculture with special reference to abiotic stress: A review. *Journal of Polymers and the Environment* **2022**, *30*, 1264–1283. https://doi.org/10.1007/s10924-021-02296-y.
5. Negi, A.; Kesari, K.K.; Chitosan nanoparticle encapsulation of antibacterial essential oils. *Micromachines* **2022**, *13*,1265. https://doi.org/10.3390/mi13081265.
6. Rossi, S.; Vigani, B.; Puccio, A.; Bonferoni, M.C.; Sandri, G.; Ferrari, F. Chitosan ascorbate nanoparticles for the vaginal delivery of antibiotic drugs in atrophic vaginitis. *Mar. Drugs* **2017**, *15*, 319. https://doi.org/10.3390/md15100319.
7. Puccio, A.; Ferrari, F.; Rossi, S.; Bonferoni, M.C.; Sandri, G.; Dacarro, C.; Grisoli, P.; Caramella, C. Comparison of functional and biological properties of chitosan and hyaluronic acid, to be used for the treatment of mucositis in cancer patients. *J. Drug Deliv. Sci. Technol.* **2011**, *21*, 241–247. https://doi.org/10.1016/S1773-2247(11)50033-4.
8. Luangtana-anan, M.; Nunthanid, J.; Limmatvapirat, S. Potential of different salt forming agents on the formation of chitosan nanoparticles as carriers for protein drug delivery systems. *J. Pharm. Investig.* **2019**, *49*, 37–44. https://doi.org/10.1007/s40005-017-0369-x.
9. Shipovskaya, A.B.; Lugovitskaya, T.N.; Zudina, I.V. Biocidal activity of chitosan aspartate nanoparticles. *Microbiology* **2023**, *92*, 75–82. https://doi.org/10.1134/S0026261722602378 DOI:10.1134/S0026261722602378.
10. Lugovitskaya, T.N.; Shipovskaya, A.B.; Shmakov, S.L.; Shipenok, X.M. Formation, structure, properties of chitosan aspartate and metastable state of its solutions for obtaining nanoparticles. *Carbohydr. Polym.* **2022**, *277*, 118773. https://doi.org/10.1016/j.carbpol.2021.118773.
11. Shipovskaya, A.B.; Gegel, N.O.; Shipenok, X.M.; Ushakova, O.S.; Lugovitskaya, T.N.; Zudina, I.V. Structure, properties and biological activity of chitosan salts with L- and D-aspartic acid. *Biol. Life Sci. Forum* **2022**, *20*, 5. https://doi.org/10.3390/IECBM2022-13399.
12. Gegel, N.O.; Zhuravleva, Yu.Yu.; Shipovskaya, A.B.; Malinkina, O.N.; Zudina, I.V. Influence of chitosan ascorbate chirality on the gelation kinetics and properties of silicon-chitosan-containing glycerohydrogels. *Polymers* **2018**, *10*, 259. https://doi.org/10.3390/polym10030259.
13. Shadrina, E.V.; Malinkina, O.N.; Khonina, T.G.; Shipovskaya, A.B.; Fomina, V.I.; Larchenko, E.Yu.; Popova, N.A.; Zyryanova, I.G.; Larionov, L.P. Formation and pharmacological activity of silicon—Chitosan-containing glycerohydrogels obtained by biomimetic mineralization. *Russ. Chem. Bull.* **2015**, *64*, 1633–1639. https://doi.org/10.1007/s11172-015-1053-9.

14. Jesus, S.; Marques, A.P.; Duarte, A.; Soares, E.; Costa, J.P.; Colaço, M.; Schmutz, M.; Som, C.; Borchard, G.; Wick, P.; et al. Chitosan nanoparticles: Shedding light on immunotoxicity and hemocompatibility. *Front. Bioeng. Biotechnol.* **2020**, *8*, 100. https://doi.org/10.3389/fbioe.2020.00100.